International Journal of Nanomedicine

Dovepress
open access to scientific and medical research

Open Access Full Text Article

ORIGINAL RESEARCH

Mimicking the Endometrial Cancer Tumor Microenvironment to Reprogram Tumor-Associated Macrophages in Disintegrable Supramolecular Gelatin Hydrogel

This article was published in the following Dove Press journal:
International Journal of Nanomedicine

Yujia Huang[1,2,*]
Qian Feng[3,*]
Huabo Jiang[1,*]
Wanding Zhou[1,2]
Jinhong Chen[2]
Jie Gao[4]
Kai Wang[1]
Xiaoping Wan[2]
Yongsheng Yu[1]

[1]Clinical and Translational Research Center, Shanghai First Maternity and Infant Hospital, Tongji University School of Medicine, Shanghai, People's Republic of China; [2]Department of Gynecology, Shanghai First Maternity and Infant Hospital, Tongji University School of Medicine, Shanghai, People's Republic of China; [3]Fujian Provincial Key Laboratory of Advanced Materials Oriented Chemical Engineering, College of Chemistry and Materials Science, Fujian Normal University, Fuzhou, People's Republic of China; [4]Institute of Translational Medicine, Shanghai University, Shanghai, People's Republic of China

*These authors contributed equally to this work

Purpose: Besides the tumor cells themselves, solid tumors are comprised of numerous cell types including infiltrating immune cells such as tumor-associated macrophages (TAMs). TAMs are vital stromal components of host immune system and play a critical role in the development of cancer. TAMs can be divided into two subtypes: M1 tumor-suppressive macrophage and M2 tumor-supportive macrophage. To better address the observations of TAMs functional performance, we describe an in vitro system that mimics the populations of TAMs infiltrated into the tumor mass by using our disintegrable supramolecular gelatin (DSG) hydrogels, which are physically crosslinked by host-guest complexations.

Materials and Methods: The host–guest interaction was adopted between the aromatic groups of gelatin and the photocrosslinkable acrylated β-cyclodextrins (Ac-β-CDs) to form the DSG hydrogels. The convenient macrophage/endometrial cancer cells heterospheroid 3D model was set up by DSG hydrogels. RT-PCR and Western blot assays were developed to evaluate the efficiencies of inducers on the macrophages. The ELISA and oxygen saturation assays were performed to measure the secretion of VEGF and consumption of oxygen of tumor and/or macrophages, respectively. To determine the antitumor effects of M2 reprogrammed macrophages in vitro and in vivo, migration assay and tumor xenograft model were used, respectively.

Results: The host-guest complexations of DSG hydrogels were controllably broken efficiently by soaking into the solution of competitive guest monomers 1-adamantanamine hydrochloride. The DSG hydrogels help IFN-γ reprogram the M2 to M1 and then decrease the tumor/M2 reprogrammed macrophage cells heterospheroid secretion of VEGF and increase the relative oxygen saturation. Significantly, the co-cultural tumor/M2 reprogrammed group from the disintegrated DSG hydrogels reduced the migration of cancer cells in vitro and the tumor growth in vivo.

Conclusion: We obtain a TAMs/tumor microenvironment-responsive 3D model based on the novel DSG hydrogels, and will be of utility in cancer therapy and drug discovery.

Keywords: supramolecular hydrogel, disintegration, host-guest complexations, tumor mimic model, tumor-associated macrophages, TAMs

Introduction

The tumor stroma consists of various cellular components that support the tumor microenvironment, including fibroblasts, endothelial, myofibroblasts, pericytes, and a diversity of immune cells.[1] Tumor cells and inflammatory tumor tissues can recruit numerous types of adaptive and innate cells, especially tumor-associated

Correspondence: Xiaoping Wan; Yongsheng Yu
Email wanxiaoping61@126.com; yongshengyu@tongji.edu.cn

http://doi.org/10.2147/IJN.S252074

macrophages (TAMs). Several recent works have indicated that TAMs content in human tumors ranges from 50% to 80%. The quantifying infiltration in medullary breast cancer is 490 macrophages/mm^2 and that in ductal carcinomas are 343 macrophages/mm^2.[2,3] High TAMs infiltration demonstrates worse relapse-free and overall survival in clinical research, emphasizing their significant in cancer prognosis and treatment.[4,5] TAMs are typically divided into two polarization phenotypes: M1 and M2 states. M1 TAMs act as potent effector cells which can suppress target tumor cells by inducing a proinflammatory response, such as TNF-α, IL-12, and IL-6.[6,7] This is in contrast to M2 TAMs that inhibit the host anticancer immune response.[8] Given the critical roles that M1 TAMs and M2 TAMs play in human tumors, the development of in vitro and in vivo models, which outline the reciprocation among M1 TAMs, M2 TAMs, and tumor cells, is of important clinical and basic interest.[9–11]

Supernatant transfer and monolayer co-culture in vitro have been used to mimic the tumor microenvironment.[12] However, both of these two models are insufficient to follow the three dimension localization of TAMs with respect to the human tumors. Hydrogels are 3D hydrophilic polymer networks which have been extensively used for studying cell–cell interactions and drug screening in many cancer models.[13–17] Hydrogels supply a distinct system to mimic environment of an in vivo tumor, for example, the metabolic gradients, the multicellular nature, and the inclusion of stromal elements such as the subordinate cell types and the extracellular matrix.[18,19] Spheroid is a kind of valuable model to mimic the tumor microenvironment in vivo.[20] Kinds of cell types including cancer cells, endothelial cells, and immune cells were incorporated to form a heterospheroid.[21,22] Tevis et al, demonstrated that the macrophage/tumor cells embedded heterospheroid model promoted TAM-like characteristics in collagen hydrogel.[20] This study demonstrated that both the three-dimensional collagen matrix and cell–cell interactions directed TAMs activity, and thus, highlighted the critical role that the local tumor microenvironment itself plays in TAMs behavior. However, reprogramming TAMs to investigate their functional performance in hydrogel is rarely studied.

Matrigel is the most extensively used hydrogel scaffolds until now, which is an extracellular matrix divided from Engelbreth-Holm-Swarm mouse sarcoma.[13,23] Although the matrigel scaffolds can sustain the multicellular breast epithelial cell spheroids in vivo, there arestillvarious limited properties, such as undefined elements and inadequate user-specified control of physicochemical.[13] To address these challenges, we develop a novel disintegration controllable supramolecular gelatin (DSG) hydrogels. Gelatin is a native protein isolated from the partial hydrolysis of collagen derived from the bones, connective tissues, and skin of animals.[24,25] Due to the good biocompatibility and abundancy, gelatin is widely used to fabricate hydrogels to mimic the extracellular matrix (ECM). For most gelatin-based hydrogels, gelatin should be chemically modified by polymerizable groups, such as vinyl groups, which complicate the process of gelatin hydrogel formation and may sacrifice partial bioactivity of gelatin.[26] Therefore, we adopt the host–guest interaction between the aromatic groups of gelatin and the modified photocrosslinkable β-cyclodextrins to form our DSG hydrogels. β-cyclodextrin (β-CD), which is widely used in the pharmaceutical industry to improve the solubility and bioavailability of hydrophobic drugs,[27] is also a common used host molecule in supramolecular chemistry.[28] Based on this novel approach, we do not need to pre-functionalize gelatin. Moreover, the weak host-guest complexation between the aromatic group and the β-CD is physically reversible. Therefore, this crosslinking can be broken by 1-adamantanamine hydrochloride (ADA), which is another kind of guest monomer showing higher binding constant with β-CD than aromatic group. In consequence, we can encapsulate cells in the biocompatible DSG hydrogels for 3D in vitro culture firstly, and then disintegrate the cell-laden DSG hydrogels to free cells for further measurements when needed.

In order to study how reprogramming M2 polarized TAMs could affect tumor cells, we set up a convenient macrophage/endometrial cancer cells Ishikawa (ISK) spheroid 3D model by gelatin DSG hydrogels. Tumor-associated macrophages are differentiated originated from the human leukemia monocytic cell line which can be differentiated into macrophages. As we all know that the cell factor interferon-γ (IFN-γ) can reprogram macrophages from M2 to M1 macrophages.[29] Co-culture systems supply a way to study the interactions between multiple macrophages and cancer cells and approve all the cells to remodel the local tumor microenvironment. M2 subtype TAMs lead to secrete of vascular endothelial growth factor (VEGF) and increase of the cancer cells migration.[30,31] The application of these models has supplied key insights into tumor-associated macrophage biology. Our study set the scene for an active area of research and will be of utility in preparing a TAMs

responsive DSG hydrogel that the TAMs can reprogram as they grow inside the hydrogels, therefore supplying a favorable mimetic of the natural extracellular matrix (ECM).

Materials and Methods

Materials

β-cyclodextrin (β-CD), hydrogen peroxide (H_2O_2) and acrylate chloride were purchased from Aladdin. Gelatin (type A, Sigma), acryloyl chloride, 2- hydroxy-4′-(2-hydroxyethoxy)-2-methylpropiophenone (I2959), and Triethylamine (TEA) were bought from Sigma-Aldrich. Acetone and Dimethyl Formamide (DMF) were bought from Thermo Fisher Scientific. Phosphate buffered saline (DPBS), penicillin, L-glutamine, Calcein AM/propidium iodide (PI), streptomycin, Trizol, and fetal bovine serum (FBS) were bought from Gibco. Both the BCA protein assay kit and RevertAid First strand cDNA synthesis kit were obtained from Thermo Fisher Scientific.

Synthesis of Acrylated β-Cyclodextrin (Ac-β-CD)

β-cyclodextrin was added into DMF to form the solution with 7% weight percentage. 5 (w/v) % TEA was then added into the β-cyclodextrin/DMF solution to act as the acid-binding agent. After the solution cooled down to 0°C, appropriate amount of acryloyl chloride was dropwise added into the above mixture. After the overnight reaction, the cloudy mixture was filtrated to obtain clear solution, and then the obtained solution was concentrated by using the vacuum rotary evaporation. The condensed solution was dripped into 30-fold volume of acetone to get white precipitate. At last, the precipitate was vacuum dried to get the product acylate β-cyclodextrin (Ac-β-CD). 1H NMR (Bruker Advance 600 MHz spectrometer) was used to define the substitution degree (SD) of the acrylate β-cyclodextrin as 1.3 (Supporting information Figure 1).

Preparation of Supramolecular Gelatin DSG Hydrogels

Gelatin and Ac-β-CD were dissolved in PBS as the certain amount, and then the photoinitiator 0.05 (w/v) % I2959 was added at 37°C. The DSG hydrogels were grouped as Gel_xCD_y (x is the concentration of gelatin, y is the concentration of Ac-β-CD). The well-mixed solution was added to molds and then the ultraviolet light (UV) was used to expose (365 nm, 10 mW/cm^2, 10 min) at 25°C to form the disintegration controllable supramolecular gelatin (DSG) hydrogels.

Rheological Measurement

Anton Paar MCR301 rheometer was used to test the rheological properties of the gelatin DSG hydrogels by using 25 mm plates at a 100 μm gap size. The samples were spread between the two plates of the rheometer homogeneously. Time sweep test was done with a 10 Hz frequency and a 0.1% strain. For the frequency sweep test, the frequency was ranged from 0.1 to 10 Hz at a fixed strain (0.1%).

Cell Culture

Ishikawa (ISK) (Sigma-Aldrich), a human endometrial adenocarcinoma, was cultured in Dulbecco's Modified Eagle Media (DMEM) added with 10% fetal bovine serum (FBS, BI, Israel) and streptomycin/penicillin (1%, 10 mg/mL streptomycin; 10,000 units/mL penicillin) (Thermo Fisher Scientific, USA). THP-1 monocytes (ATCC, USA) were cultured at 37°C in a 5% CO_2 incubator in Roswell Park Memorial Institute (RPMI) 1640 (BI, Israel) with 10% fetal bovine serum (FBS) and streptomycin/penicillin (1%, 10 mg/mL streptomycin; 10,000 units/mL penicillin) (Thermo Fisher Scientific, USA). THP-1 monocytes were supplemented with 100 ng/mL 2-Acetoxy-1-methoxypropane (PMA) for 48 hours to induce THP-1 M0 macrophages both in 2D and 3D culture systems.

Spheroid Formation and Disintegration

For the spheroid formation, the method was used as previously published method.[22,32] Briefly, 5×10^5/mL THP-1 M0 cells were added to agarose-coated 96-well plates with 1×10^6/mL ISK cells, and then performed a centrifugation at 1000 g for 10 min to form the heterospheroid. The 10C5M model (cancer cells/macrophage cells), which has been proved promoting TAM-like characteristics, was formed in DSG hydrogels during the spheroid embedding as previously described by Grinstaff et al.[20] The single kind of cells spheroid model (cancer cells, M0 macrophage cells, M1 type macrophage cells, or M2 type macrophage cells) was also created in 96-well plates as described above. RPMI 1640 with 10% FBS (BI, Israel) and streptomycin/penicillin (1%, 10,000 mg/mL streptomycin; 10,000 IU/mL penicillin) was added for both in 2D and 3D culture systems (Supporting information Figure 2A). The cultural medium was changed every two days during the culture in vitro. Viability was detected on

3-dimensional cell culture trials by Calcein AM and propidium iodide (PI). For the spheroid disintegration, 1 μM 1-adamantanamine hydrochloride (ADA) was added to break the crosslinking of DSG for 5 min at 37°C. The released cells were centrifuged to collect for the further use (Supporting information Figure 2B).

Western Blot

M0 macrophages were incubated by PBS (for control), IFN-γ (for M1 type), or IL-4 (for M2 type) at different concentrations from 0, 20, 50, to 100 ng/mL both in 2D and 3D systems for 24 h. To reprogram M2 type macrophages to M1 type, IFN-γ (100 ng/mL) was added to the induced M0 macrophages above for 24 h. Then, the cells were disrupted on ice in lysis buffer containing 50 mM PBS (pH 8.0), 1% (v/v) Triton-X 100, 1 mM magnesium chloride, 150 mM NaCl, and the protease inhibitor cocktail phenylmethylsulfonyl fluoride (PMSF) (Roche, Shanghai, China). The BCA Protein Assay kit (Thermo Fisher Scientific, USA) was used to analyze the protein content quantitatively. Each sample was separated on 10% polyacrylamide gel by SDS PAGE and transferred to a nitrocellulose membrane. Membranes were incubated in a blocking buffer containing 5% (w/v) bovine serum albumin, 0.01 M Tris-buffered saline (TBS), 0.1% (v/v) Tween 20 (TBS-T) for 4 h at room temperature. The primary antibodies (iNOS, Arg1, CD68, or GAPDH) were incubated overnight at 4°C, and then incubated with a homologous 1:10,000-diluted secondary HRP-antibody for 2 h at room temperature. The chemiluminescence reaction was performed using an enhanced chemiluminescence (ECL).

Quantitative Real-Time Polymerase Chain Reaction (RT-PCR)

The mRNA expression levels of CD68 and iNOS in M0, M2, M2 reprogrammed, and M1 macrophage were detected by RT-PCR after 24h induction, respectively. Briefly, total RNA was divided from the macrophages with Trizol reagent (Life technology, Shanghai, China) and the Reverse Transcription System kit (TAKARA, Dalian, China) was used to transcribe the first-strand cDNA from RNA reversely. RT-PCR reactions were measured using a Sequence Detection System AppliedBiosystems 7500 (Applied Biosystems, USA).

The primers used as below:

iNOS-Forward:5′-GAACAGCCAGCTCATCCGATA-3′,

Reverse:5′-CCCAAGCTCAATGCACAACTT-3′;

CD68-Forward:5′-CCAGCTGTCCACCTCGACCT-3′,

Reverse:5′-GATGAGAGGCAGCAAGATGGAC-3′

β-actin-Forward:5′-TGCCGACAGGATGCAGAAG-3′,

Reverse:5′-GCCGATCCACACGGAGTACT-3′.

ELISA Assay

After culturing with 2D and 3D hydrogel model after 24 h induction, a human VEGF ELISA Kit (Rockland, USA) was used to measure the concentration of VEGF in the supernatants of the co-culture Ishikawa and TAMs systems according to the manufacturer's instructions.

Oxygen Saturation

The SpectraMax M5 plate reader (Molecular Devices, USA) was used to detect the oxygen saturation of every group in 96 well oxoplates with 100 μL culture medium (PreSens Precision Sensing, Germany). Data were collected in accordance with the manufacturer's instructions. All the obtained data points that surpassed two standard deviations from the averages were kicked as outliers.

ISK Cell Migration Assay

ISK, ISK/M1, ISK/M2, or ISK/M2 reprogrammed cells were encapsulated in DSG hydrogel and cultured as described above, and then, retrieved from the hydrogels by ADA. Subsequently, the cells were collected by performing a concentration. The polycarbonate Transwell membranes of 8 μm pores (Corning, USA) were used. 600 μL of medium with 10% FBS was added to the low chambers of the Transwell. 5×10^4 cells were placed in the top chambers in 200 μL of FBS free medium. The whole plate was incubated in 5% CO_2 at 37°C for 16 h. Then, the attached cells on the upper side of the membrane were wiped off. Methanol and crystal violet were used to fix or stain the cells, respectively. Under a microscope with a 20×objective, the stained cells that had migrated to the bottom side of the membrane were counted. 5 central fields were randomly chosen for each group. The average numbers of migrated cells per group were analyzed.

In vivo Antitumor Activity

All animal experiments were carried out in agreement with the National Institutes of Health (NIH) requirements for the care and use of laboratory animals and approved by the Tongji University Animal Study Committee. The released cells from each group were transplanted into the rear of six-week-old BABL/c nude mice (5×10^6 cells) subcutaneously.

Five mouse each group. Calipers were used to measure the tumor size, and the tumor volume was calculated by the formula: (V) = a×b^2×0.5 (a: the min diameter; b: the max diameter). Mice were sacrificed 4–5 weeks later.

Results and Discussions

Fabrication of DSG Hydrogels

Firstly, we synthesized Ac-β-CD as described in our previous study.[33] Just by dissolving the natural gelatin and Ac-β-CD in phosphate-buffered saline buffer simultaneously, pre-organized host-guest macromer was efficiently formed driven by the host–guest interaction between the aromatic residues of gelatin backbone (phenylalanine, tyrosine, and tryptophan) and Ac-β-CDs (Figure 1A).[34,35] Then, exposing the solution of host-guest macromer to UV can initiate the polymerization of the Ac-β-CDs leading to the formation of DSG hydrogels (Figure 1A and B). As shown in Figure 2A, the rheological time sweep test demonstrated that both the storage modulus and the loss modulus of pure gelatin hydrogel (Gel8CD0 group) are significantly lower than the hydrogel with the addition of Ac-β-CDs (Gel8CD4 and Gel8CD10 groups). Moreover, with the increasing of the Ac-β-CDs concentration, the modulus of hydrogels was increasing. These results demonstrate that the DSG gelatin hydrogel is well obtained. Furthermore, Figure 2B shows the gelation time of the DSG hydrogels was about 90s (gelatin point: G' > G"). The rheological frequency sweep (Figure 2C) showed the frequency-dependent property of DSG hydrogels, which proved the physically reversible crosslinkings of DSG hydrogels. Furthermore, Figure 2D shows that after the addition of ADA, the DcS hydrogels (Gel8CD10 with ADA groups) converted to liquid (G' < G') at 37°C. This is because that the binding constant between β-CDs and such aromatic residues is relatively lower (Ka~10^2 M^{-1}) than that between β-CDs and ADAs (Ka~10^5 M^{-1}). After the addition of the ADA solution to the DSG hydrogels, the small ADA molecules would complex with β-CDs to unlock the crosslinking between the aromatic groups of gelatin backbones and the β-CDs resulting in the disintegration-controllable of DSG hydrogels. Therefore, based on the special disintegration-controllable property of our DSG hydrogels, we are able to encapsulate tumor-associated macrophages (TAMs) and Tumor cells into the DSG hydrogels for 3D in vitro co-culture firstly. Then, the cell-laden DSG hydrogels can be

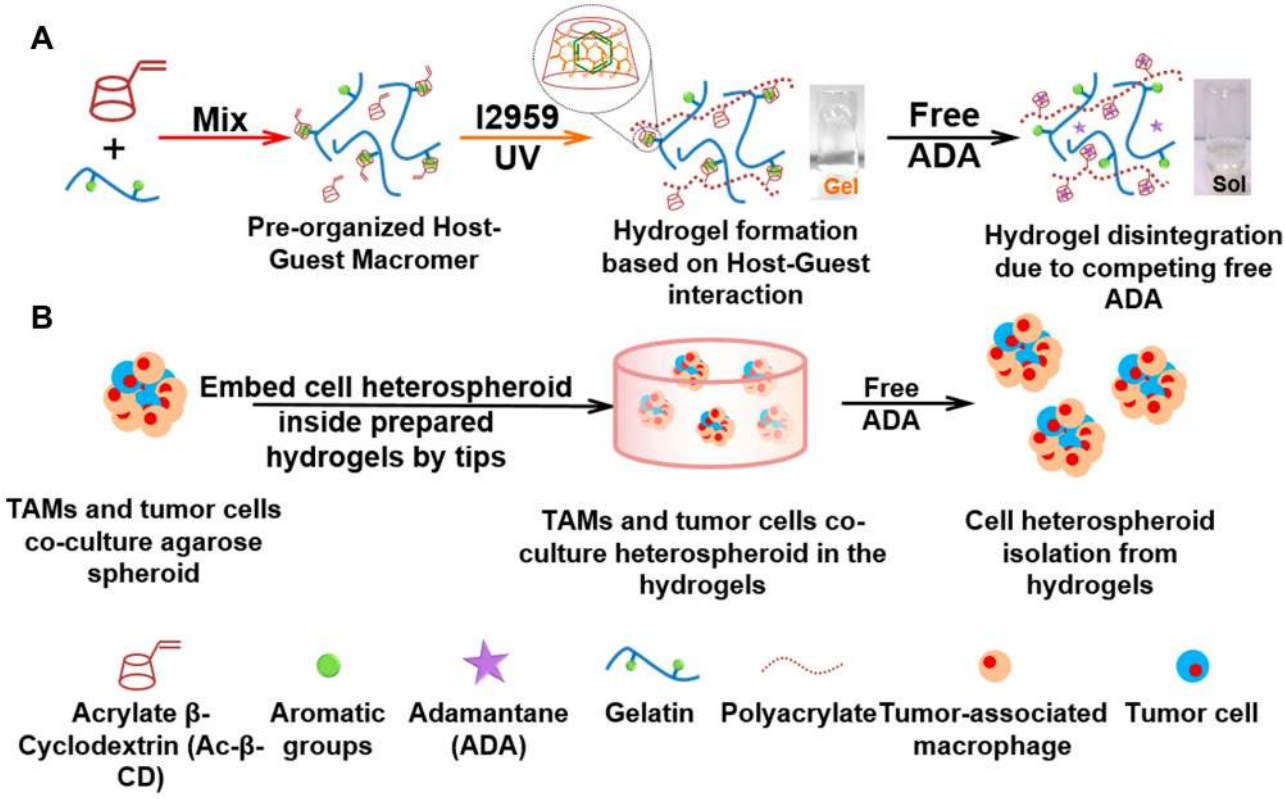

Figure 1 (**A**) Illustration of the formation and disintegration process of the DSG hydrogels. (**B**) Illustration of the formation of TAMs/tumor cells model.

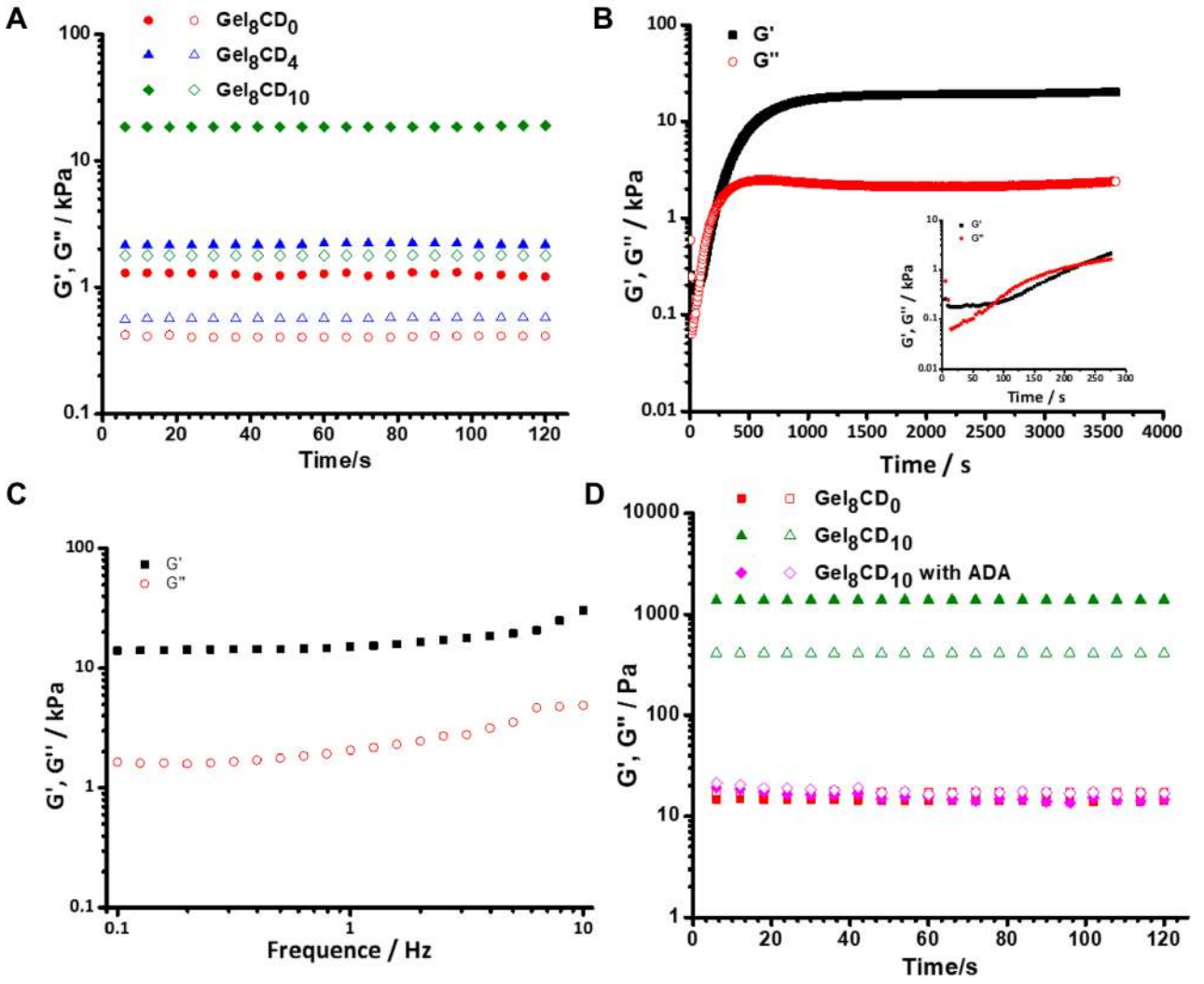

Figure 2 The properties of DSG hydrogels. (**A**) The rheological time sweep test for DSG hydrogels with different concentration of gelatin and Ac-β-CD at 25°C. (The solid symbols represent storage modulus (G') and the hollow symbols represent loss modulus (G")). (**B**) The gelation time test for Gel8CD10 hydrogel group at 25°C. (Insert graph: the enlarged view for the region of 0–300s). (**C**) The rheological frequency sweep of Gel_8CD_{10} hydrogel group at 25°C. (**D**) The rheological time sweep test for DcS hydrogels before and after the addition of ADA at 37°C.

disintegrated by immersing into the ADA solution to isolate the encapsulated cells from the DSG hydrogels for further detection (Figure 1B). Compared to the PBS treated control cells, the cell viability assay demonstrated the used ADA had non-cytotoxicity on cells (Supporting information Figure 2C).

Polarization of Macrophages into Different Subtypes in 2D and 3D Systems

The classically activated type 1 (M1) and the alternatively activated type 2 (M2) are two major polarization states in macrophages. The expression of iNOS is much higher in M1 macrophages, while the Arg-1 is highly expressed in macrophages M2.[36–39] In 2D culture system after 24 h induction, Western blot results showed that the expression of iNOS was up-regulated after IFN-γ induction of THP-1 M0 cells (termed M1 type macrophages) compared with control cells and Arg-1 expression was up-regulated after IL-4 induction (termed M2 type macrophages), respectively (Figure 3A and B). In order to analysis of the induction efficiency of polarization in 3D systems after 24 h induction, the macrophage cells released by ADA from the DSG hydrogel were also collected and detected by Western blot. As we expected, the polarization of macrophages into both M1 and M2 subtypes was high efficient after 24 h of the induction by IFN-γ and IL-4, respectively (Figure 3C and D). These demonstrated that the M0, M1, and M2 subtype macrophages were induced efficiently both in 2D and 3D

hydrogels. The polarization level increasing responded to the concentrations of inducers from 0 to 100 ng/mL in a dose-dependent manner both in 2D and 3D systems, respectively. The final concentration of IFN-γ or IL-4 at 100 ng/mL was used to perform the followed experiments. To further characterize the reprogram of M2 macrophage subtype in DSG hydrogel, we detected the expression of markers that are generally responsible for the M1 responses in polarized macrophages by real-time PCR and Western blot. The M0 macrophage cells were induced to the M2 polarized macrophage firstly, and then, the IFN-γ was added to reprogram M2 macrophage subtype in DSG hydrogels. The CD68, another expression of recognized M1 macrophage marker was also measured.[40,41] As shown in Figure 4A, the mRNAs (both iNOS and CD68) expression levels of M2 reprogrammed macrophage cells released from DSG hydrogels were significantly up-regulated after 24 h IFN-γ induction compared with M0 and M2 macrophage cells. The similar results of proteins expression were obtained from the Western blot (Figure 4B and C). These indicated that reprogramming of M2 type macrophages to M1 was efficient after 24 h induction in 3D DSG hydrogels. Significantly, the microscope results of Calcein AM/PI cell viability assay showed all the cells of the different groups

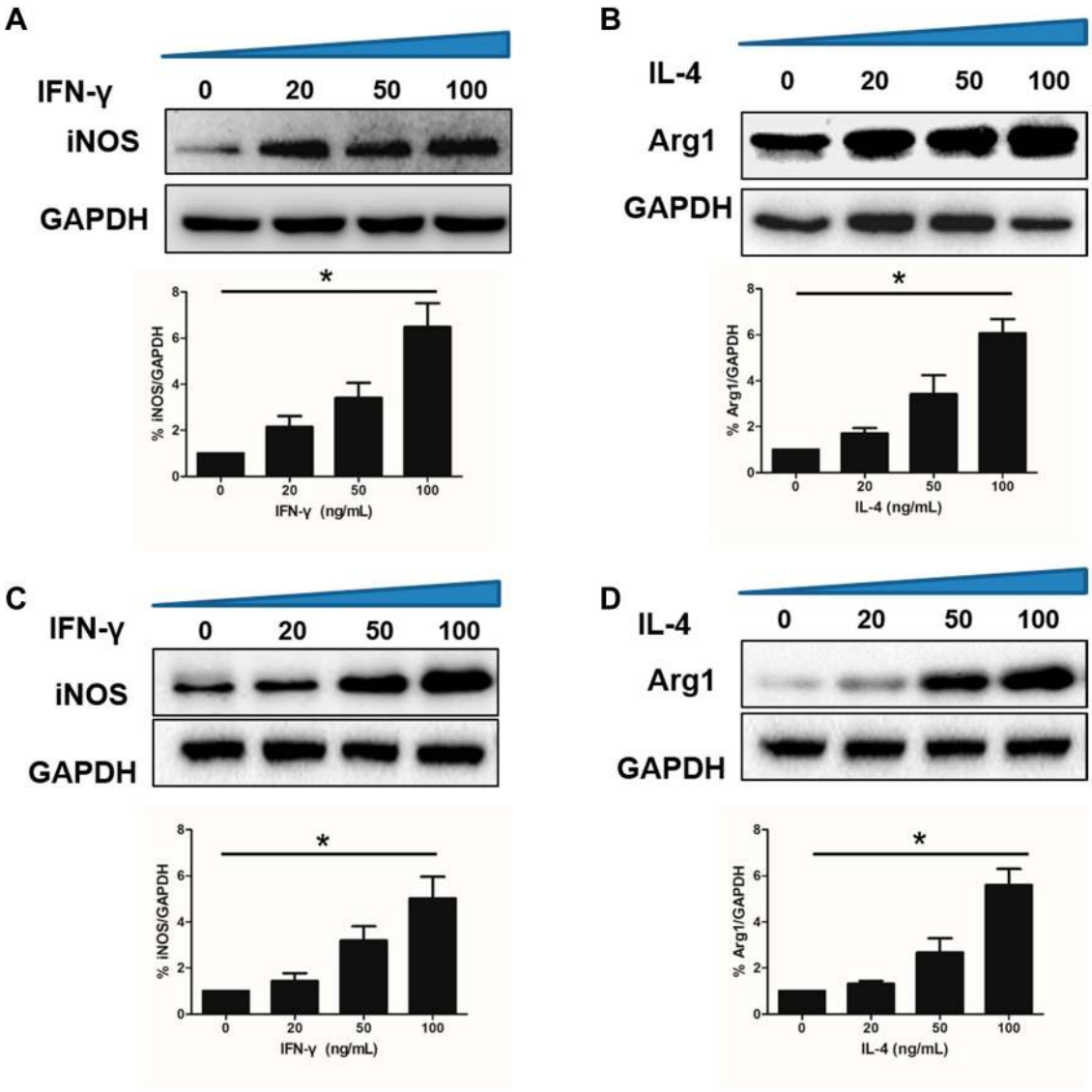

Figure 3 Protein expression levels of THP-1 M0 cells polarization for 24 h in the presence of IFN-γ or IL-4, respectively. (**A**) Western blot analysis of iNOS (upper), relative expression of iNOS (lower) in 2D. (**B**) Western blot analysis of Arg1 (upper), relative expression of Arg1 (lower) in 2D. (**C**) Western blot analysis of iNOS (upper), relative expression of iNOS (lower) in 3D. (**D**) Western blot analysis of Arg1 (upper), relative expression of Arg1 (lower) in 3D. Data are presented as means ± standard deviations (n = 3). *$p < 0.01$.

remain high viability (green fluorescence) and well spreading with the surrounding hydrogel matrix (Figure 4D). These proved that the hydrogel showed good biocompatibility and non-cytotoxicity.

Reprogram M2 Macrophages Decreases the VEGF and Increases Oxygen Saturation in 3D Compared with 2D Systems

The macrophage/cancer cells heterospheroid (10C5M) model exposes macrophages to a tumor microenvironment more according to that found within an in vivo tumor.[20] We established and used this macrophage/cancer cells heterospheroid (10C5M) model with DSG hydrogels in this study. In malignant tumors, M2 TAM macrophages promote tumor cell growth and survival by secretion of many cytokines such as vascular endothelial growth factor (VEGF).[5] Moreover, VEGF might contribute to M2 TAM accumulation in the tumor microenvironment.[42] The expression of VEGF was measured at the protein level by ELISA after 24 h induction both in 2D and 3D systems. Compared with 2D model system, the 3D model exhibited dramatic release of VEGF both in ISK alone and ISK/M2 complex, while the opposite results were obtained both in ISK/M1 and ISK/M2 reprogrammed complex (Figure 5A). Although multiple studies reported that IFN-γ performed anticancer effect, as shown in Figure 5A, IFN-γ treated ISK cells secreted a higher concentration of VEGF than ISK/M2 reprogrammed group, especially in 3D DSG hydrogels. With the aim of evaluating the metabolic rate, we used the oxoplates to assess the partial pressure of oxygen in the hydrogels. Then, we observed that the percent oxygen saturation via sensors of oxoplates of the 3D cell model system. The

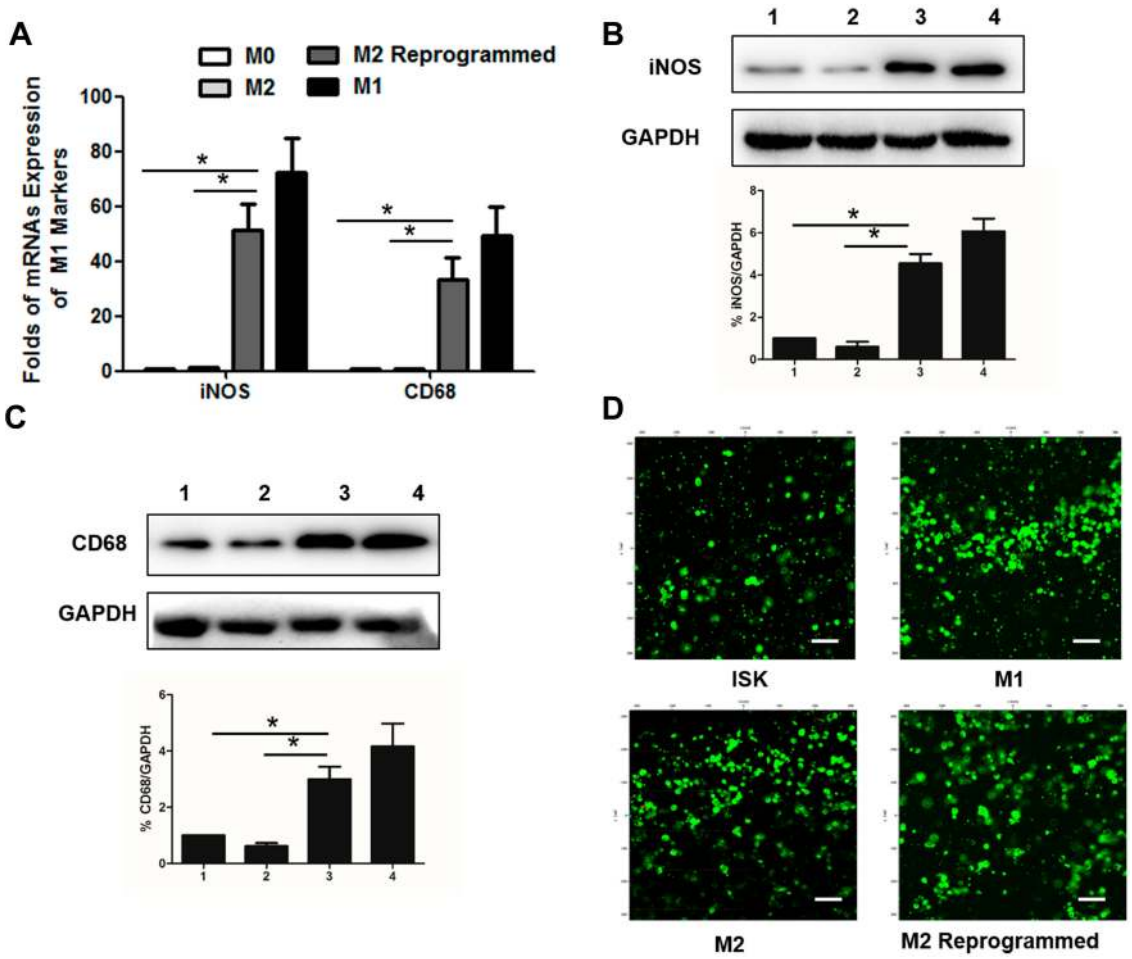

Figure 4 Relative M1 subtype markers expression of macrophage cells and cell viability in DSG hydrogels. (**A**) Relative iNOS and CD68 mRNAs expression of macrophage cells. (**B**) Relative iNOS protein expression of macrophage cells (1:M0; 2:M2; 3:M2 Reprogrammed; 4:M1). (**C**) Relative CD68 protein expression of macrophage cells (1:M0; 2:M2; 3:M2 Reprogrammed; 4:M1). (**D**) Cell viability staining (Green: Live; Red: Dead) of the cells-laden DSG hydrogels after 3 days. Scale bar:100 μm. Data are presented as means ± standard deviations (n = 3). *$p < 0.001$.

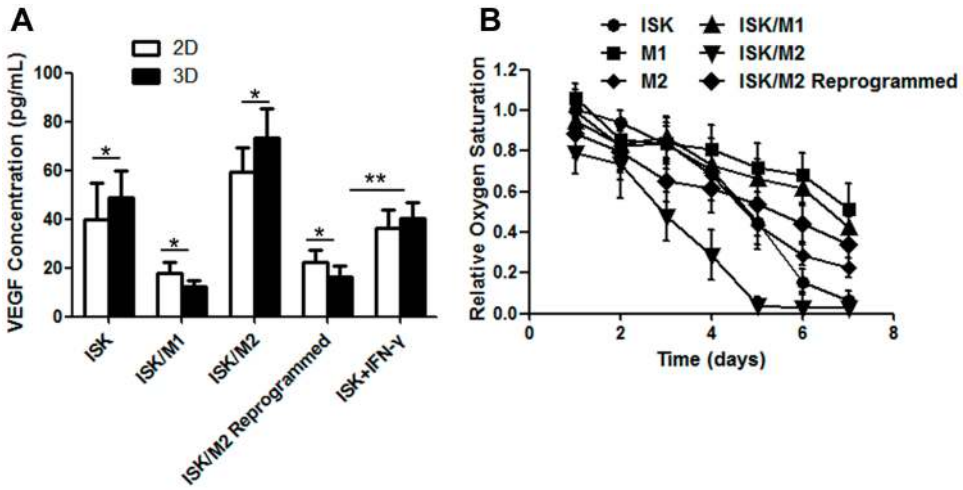

Figure 5 VEGF concentration measured by ELISA from the five models (**A**). The qualified oxygen saturation via oxoplates sensors of the 3D cell model system. The relative oxygen level for the six different complexes using 5×10^3 macrophages and/or 1×10^4 tumor cells. The relative oxygen saturation of co-culture growth in spheroid systems (**B**). Data are presented as means ± standard deviations (n = 3).*p< 0.05, **p< 0.01.

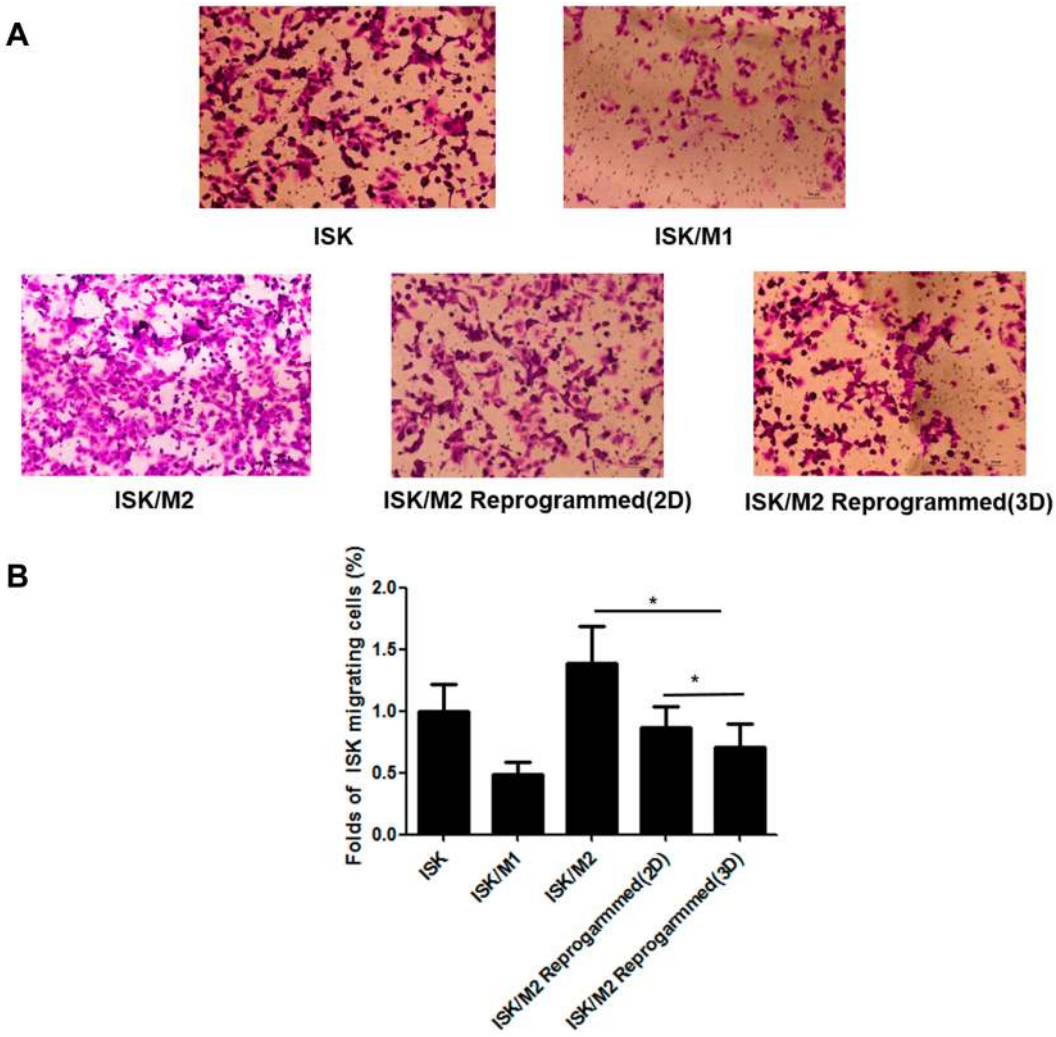

Figure 6 Reprogram M2 macrophages inhibited cell migration in a Transwell assay. The stained cells that accumulating at the bottom side of the Transwell membrane observed under a microscope (**A**). Quantification of the migrating cancer cells in different models (**B**). Scale bar:100μm. Data are presented as means ± standard deviations (n = 3). *p < 0.01.

qualified oxygen level for the six different complexes (ISK cancer cell spheroid alone, M1, M2, ISK/M1, and ISK/M2 reprogrammed complex models) using 5×10^3 macrophages and/or 1×10^4 tumor cells is shown in Figure 5B. The percent oxygen levels decreased gradually from 100% to almost 10% at the end of five days in the ISK/M2 model. The oxygen consumption of the ISK cancer cell alone model followed the trajectory of the ISK/M1 model until day four when consumption improved and oxygen levels rapidly declined. This pattern was mirrored by the ISK/M2 model, where the rapid decline in percent oxygen saturation occurred at day one, beginning at an initial oxygen level of only 80% and following with an exponential decay. However, the ISK/M2 reprogrammed model slowly consumed oxygen from day one to seven, proofing that M2 reprogrammed decreased the proliferation of ISK. These indicated that ISK/M2 complex in hydrogel could mimic the real situation in vivo.

Reprogram M2 Macrophages Decreases the Tumor Cells Migration

Cell migration serves as a critical role in various biological phenomena including cancer progression and tissue morphogenesis. Due to the capability of tumor cells migration is closely related to human tumor metastasis and progression,[43–46] we next examined whether reprogramming M2 macrophages would lead to the prohibition of ISK cancer cells migration. Cells on the top side of membrane are prone to migrate to serum-containing culture medium and accumulate at the bottom side of the membrane. The cells migration capability was measured by the quantification of the cells number accumulating at the bottom side of the membrane. After 24

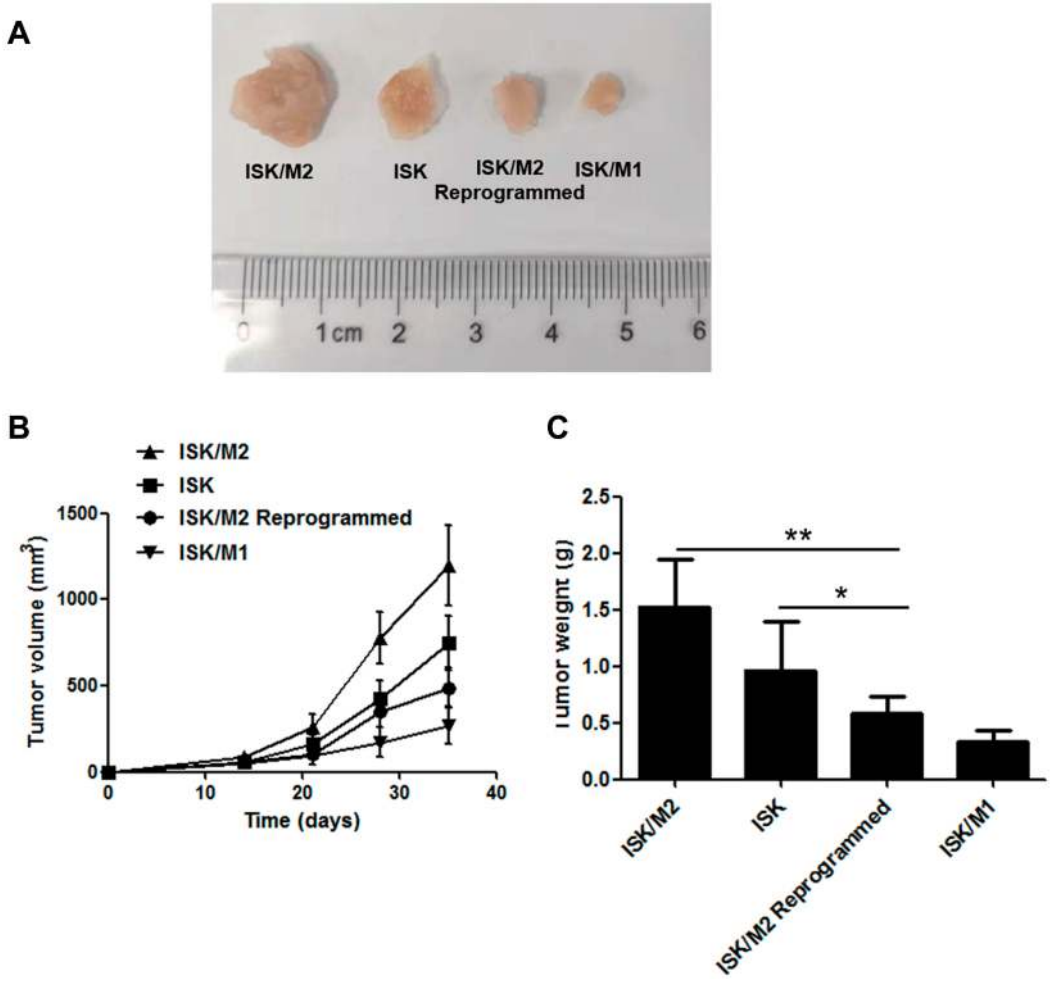

Figure 7 Reprogram M2 macrophages from the 3D hydrogels reducing tumor growth in vivo. The released cells were transplanted subcutaneously into the rear of six-week-old BABL/c nude mice. Photographs of the dissected xenograft tumors from various groups treated as indicated (**A**). Kinetics of tumor growth from various groups treated as indicated (**B**). Statistical analysis of the tumor weight of different models (**C**). Data are presented as means ± standard deviations (n = 5). *$p < 0.05$, **$p<0.01$.

h induction in every model, the cells released from the hydrogel dissolved by the ADA were collected and plated on the top side of Transwell chamber for 18 h. The results showed that the ISK/M2 cells promoted the percentage of the migrating cells compared with other groups. Significantly, compared with ISK/M2 model (~130%), we observed that the ISK cells from ISK/M2 reprogrammed model reduced the percentage of the migrating cells (~50%) (Figure 6A and B). Compared with migrating cells of ISK/M2 Reprogrammed in 2D system (~80%), the cells in 3D hydrogel showed lower migrating rate (~50%). The proliferation assay showed the similar results as the migration assay (Supporting information Figure 2D). These results illustrated that the reprogrammed macrophages have anti-tumorigenic functions and this disintegration-controllable 3D system is a useful tool to mimic the tumor microenvironment.

Reprogram M2 Macrophages from the 3D Hydrogel Reduces Tumor Growth in vivo

We next examined whether the therapeutic effect was mainly contributed to the TAM reprogramming by examining the tumor volume of different groups (five mouse each group) in vivo. After 24 h induction, the released cells from the disintegration-controllable 3D hydrogel were subcutaneously injected into the BALB/c nude mice. The tumor volume was determined every 7 days for up to 35 days. It is expected that the ISK/M1 group showed a maximum inhibition effect of tumor growth compared with the other groups. The inhibition of tumor growth by the ISK/M2 reprogrammed group was more substantial, with a dramatic suppression in tumor volume and weight compared with the ISK or ISK/M2 groups (Figure 7A–C). These indicated that the DSG degradable hydrogels could mimic the endometrial cancer tumor microenvironment well in vivo.

Conclusions

We present a disintegration-controllable supramolecular gelatin hydrogel which can mimic the endometrial cancer tumor microenvironment in vivo. The DSG hydrogels heterospheroids summarized VEGF-based paracrine interactions, increased in oxygen consumption, promoted tumor growth, and secreted cytokines compatible with the polarization of M2 TAMs. This DSG hydrogels heterospheroid exposes TAMs to a microenvironment more according to that discovered in vivo tumor, thus decreasing the need for exogenous agents which often used to maintain M2 polarization. Rather, it is the synergistic combination of co-culture TAMs/tumor cells proximity and interactions present with the IFN-γ that result in M2 TAM reprogramming and inhibiting the tumor cells progression. In conclusion, we report TAMs/tumor cells interactions within the context of a motivated tumor stroma and supply the good use of in vitro heterospheroid and diffusely embed systems by DSG hydrogels as models of endometrial cancer infiltrated with TAMs for future application in cancer therapy, agent mechanism studies, and drug delivery.

Funding

This work was financially supported by the National Natural Science Foundation of China (81902622 and 31900963), the Shanghai Pujiang Program (18PJ1409400), the Scientific Research Foundation of Shanghai Municipal Commission of Health and Family Planning (20174Y0218), and The Fifth Round of Fujian Health Education Joint Key Project (2019-WJ-22).

Disclosure

The authors declare that they have no competing interests.

References

1. Orimo A, Weinberg RA. Stromal fibroblasts in cancer: a novel tumor-promoting cell type. *Cell Cycle*. 2006;5(15):1597–1601. doi:10.4161/cc.5.15.3112
2. Bouma-ter Steege JC, Baeten CI, Thijssen VL, et al. Angiogenic profile of breast carcinoma determines leukocyte infiltration. *Clin Cancer Res*. 2004;10:7171–7178. doi:10.1158/1078-0432.CCR-04-0742
3. Sica A, Larghi P, Mancino A, et al. Macrophage polarization in tumour progression. *Semin Cancer Biol*. 2008;18(5):349–355. doi:10.1016/j.semcancer.2008.03.004
4. Zhang Y, Cheng S, Zhang M, et al. High-infiltration of tumor-associated macrophages predicts unfavorable clinical outcome for node-negative breast cancer. *PLoS One*. 2013;8(9):e76147. doi:10.1371/journal.pone.0076147
5. Tsutsui S, Yasuda K, Suzuki K, Tahara K, Higashi H, Era S. Macrophage infiltration and its prognostic implications in breast cancer: the relationship with VEGF expression and microvessel density. *Oncol Rep*. 2005;14:425–431.
6. Biswas SK, Mantovani A. Macrophage plasticity and interaction with lymphocyte subsets: cancer as a paradigm. *Nat Immunol*. 2010;11(10):889–896. doi:10.1038/ni.1937
7. Solinas G, Germano G, Mantovani A, Allavena P. Tumor-associated macrophages (TAM) as major players of the cancer-related inflammation. *J Leukoc Biol*. 2009;86:1065–1073. doi:10.1189/jlb.0609385
8. Martinez FO, Helming L, Gordon S. Alternative activation of macrophages: an immunologic functional perspective. *Annu Rev Immunol*. 2009;27:451–483. doi:10.1146/annurev.immunol.021908.132532
9. Boissonnas A, Laviron M. Ontogeny of tumor-associated macrophages. *Front Immunol*. 2019;10:1799. doi:10.3389/fimmu.2019.01799

10. Han S, Wang W, Wang S, et al. Multifunctional biomimetic nanoparticles loading baicalin for polarizing tumor-associated macrophages. *Nanoscale*. 2019;11(42):20206–20220. doi:10.1039/C9NR03353J
11. Ovais M, Guo M, Chen C. Tailoring nanomaterials for targeting tumor-associated macrophages. *Adv Mater*. 2019;31(19):e1808303. doi:10.1002/adma.201808303
12. Solinas G, Schiarea S, Liguori M, et al. Tumor-conditioned macrophages secrete migration-stimulating factor: a new marker for M2-polarization, influencing tumor cell motility. *J Immunol*. 2010;185(1):642–652. doi:10.4049/jimmunol.1000413
13. Tam RY, Smith LJ, Shoichet MS. Engineering cellular microenvironments with photo- and enzymatically responsive hydrogels: toward biomimetic 3D cell culture models. *Acc Chem Res*. 2017;50(4):703–713. doi:10.1021/acs.accounts.6b00543
14. Yu Y, Li S, Wang K, Wan X. A PDZ protein MDA-9/Syntenin: as a target for cancer therapy. *Comput Struct Biotechnol J*. 2019;17:136–141. doi:10.1016/j.csbj.2019.01.002
15. Yue L, Wang S, Wulf V, Willner I. Stiffness-switchable DNA-based constitutional dynamic network hydrogels for self-healing and matrix-guided controlled chemical processes. *Nat Commun*. 2019;10(1):1–10. doi:10.1038/s41467-019-12697-2
16. Roth AD, Lama P, Dunn S, Hong S, Lee M-Y. Polymer coating on a micropillar chip for robust attachment of PuraMatrix peptide hydrogel for 3D hepatic cell culture. *Mater Sci Eng C*. 2018;90:634–644. doi:10.1016/j.msec.2018.04.092
17. Shen Y, Abaci HE, Krupsi Y, Weng L, Burdick JA, Gerecht S. Hyaluronic acid hydrogel stiffness and oxygen tension affect cancer cell fate and endothelial sprouting. *Biomater Sci*. 2014;2:655–665. doi:10.1039/c3bm60274e
18. Campiglio CE, Bidarra SJ, Draghi L, Barrias CC. Bottom-up engineering of cell-laden hydrogel microfibrous patch for guided tissue regeneration. *Mater Sci Eng C*. 2020;108:110488. doi:10.1016/j.msec.2019.110488
19. Javanbakht S, Namazi H. Doxorubicin loaded carboxymethyl cellulose/graphene quantum dot nanocomposite hydrogel films as a potential anticancer drug delivery system. *Mater Sci Eng C*. 2018;87:50–59. doi:10.1016/j.msec.2018.02.010
20. Tevis KM, Cecchi RJ, Colson YL, Grinstaff MW. Mimicking the tumor microenvironment to regulate macrophage phenotype and assessing chemotherapeutic efficacy in embedded cancer cell/macrophage spheroid models. *Acta Biomater*. 2017;50:271–279. doi:10.1016/j.actbio.2016.12.037
21. Ho DN, Kohler N, Sigdel A, et al. Penetration of endothelial cell coated multicellular tumor spheroids by iron oxide nanoparticles. *Theranostics*. 2012;2:66–75. doi:10.7150/thno.3568
22. Lu HF, Chua K-N, Zhang P-C, et al. Three-dimensional co-culture of rat hepatocyte spheroids and NIH/3T3 fibroblasts enhances hepatocyte functional maintenance. *Acta Biomater*. 2005;1:399–410. doi:10.1016/j.actbio.2005.04.003
23. Kleinman HK, Martin GR. Matrigel: basement membrane matrix with biological activity. *Semin Cancer Biol*. 2005;15(5):378–386. doi:10.1016/j.semcancer.2005.05.004
24. Noshadi I, Hong S, Sullivan KE, et al. In vitro and in vivo analysis of visible light crosslinkable gelatin methacryloyl (GelMA) hydrogels. *Biomater Sci*. 2017;5(10):2093–2105. doi:10.1039/C7BM00110J
25. Yao M, Gao F, Xu R, Zhang J, Chen Y, Guan F. A dual-enzymatically cross-linked injectable gelatin hydrogel loaded with BMSC improves neurological function recovery of traumatic brain injury in rats. *Biomater Sci*. 2019;7(10):4088–4098. doi:10.1039/C9BM00749K
26. Lin R-Z, Chen Y-C, Moreno-Luna R, Khademhosseini A, Melero-Martin JM. Transdermal regulation of vascular network bioengineering using a photopolymerizable methacrylated gelatin hydrogel. *Biomaterials*. 2013;34(28):6785–6796. doi:10.1016/j.biomaterials.2013.05.060
27. Davis ME, Brewster ME. Cyclodextrin-based pharmaceutics: past, present and future. *Nat Rev Drug Discov*. 2004;3(12):1023–1035. doi:10.1038/nrd1576
28. Kakuta T, Takashima Y, Nakahata M, Otsubo M, Yamaguchi H, Harada A. Preorganized hydrogel: self-healing properties of supramolecular hydrogels formed by polymerization of host-guest-monomers that contain cyclodextrins and hydrophobic guest groups. *Adv Mater*. 2013;25(20):2849–2853. doi:10.1002/adma.201205321
29. Wang Y, Lin Y, Qiao S, et al. Polymeric nanoparticles promote macrophage reversal from M2 to M1 phenotypes in the tumor microenvironment. *Biomaterials*. 2017;112:153–163. doi:10.1016/j.biomaterials.2016.09.034
30. Genin M, Clement F, Fattaccioli A, Raes M, Michiels C. M1 and M2 macrophages derived from THP-1 cells differentially modulate the response of cancer cells to etoposide. *BMC Cancer*. 2015;15(1):577. doi:10.1186/s12885-015-1546-9
31. Xu WC, Dong X, Ding J, et al. Nanotubular TiO2 regulates macrophage M2 polarization and increases macrophage secretion of VEGF to accelerate endothelialization via the ERK1/2 and PI3K/AKT pathways. *Int J Nanomedicine*. 2019;14:441. doi:10.2147/IJN.S188439
32. Ivascu A, Kubbies M. Rapid generation of single-tumor spheroids for high-throughput cell function and toxicity analysis. *J Biomol Screen*. 2006;11(8):922–932. doi:10.1177/1087057106292763
33. Feng Q, Xu J, Zhang K, et al. Dynamic and cell-infiltratable hydrogels as injectable carrier of therapeutic cells and drugs for treating challenging bone defects. *ACS Cent Sci*. 2019;5(3):440–450. doi:10.1021/acscentsci.8b00764
34. Jana M, Bandyopadhyay S. Molecular dynamics study of β-cyclodextrin–phenylalanine (1:1) inclusion complex in aqueous medium. *J Phys Chem B*. 2013;117:9280–9287. doi:10.1021/jp404348u
35. Ma M, Xu S, Xing P, Li S, Chu X, Hao A. A multistimuli-responsive supramolecular vesicle constructed by cyclodextrins and tyrosine. *Colloid Polym Sci*. 2015;293(3):891–900. doi:10.1007/s00396-014-3424-4
36. Biswas SK, Allavena P, Mantovani A. Tumor-associated macrophages: functional diversity, clinical significance, and open questions. *Semin Immunopathol*. 2013;35(5):585–600. doi:10.1007/s00281-013-0367-7
37. Liu L, Yi H, He H, Pan H, Cai L, Ma Y. Tumor associated macrophage-targeted microRNA delivery with dual-responsive polypeptide nanovectors for anti-cancer therapy. *Biomaterials*. 2017;134:166–179. doi:10.1016/j.biomaterials.2017.04.043
38. Mantovani A, Sica A, Sozzani S, Allavena P, Vecchi A, Locati M. The chemokine system in diverse forms of macrophage activation and polarization. *Trends Immunol*. 2004;25(12):677–686. doi:10.1016/j.it.2004.09.015
39. Parayath NN, Parikh A, Amiji MM. Repolarization of tumor-associated macrophages in a genetically engineered nonsmall cell lung cancer model by intraperitoneal administration of hyaluronic acid-based nanoparticles encapsulating microRNA-125b. *Nano Lett*. 2018;18(6):3571–3579. doi:10.1021/acs.nanolett.8b00689
40. Holness CL, Simmons DL. Molecular cloning of CD68, a human macrophage marker related to lysosomal glycoproteins. *Blood*. 1993;81(6):1607–1613. doi:10.1182/blood.V81.6.1607.1607
41. Shi Y, Zong Z, Zou J, et al. M1 macrophages induce PD-L1 expression in hepatocellular carcinoma cells through IL-1β signaling. *Front Immunol*. 2019;10:1643. doi:10.3389/fimmu.2019.01643
42. Duluc D, Delneste Y, Tan F, et al. Tumor-associated leukemia inhibitory factor and IL-6 skew monocyte differentiation into tumor-associated macrophage-like cells. *Blood*. 2007;110(13):4319–4330. doi:10.1182/blood-2007-02-072587
43. Hanahan D, Weinberg RA. The hallmarks of cancer. *Cell*. 2000;100(1):57–70. doi:10.1016/S0092-8674(00)81683-9
44. Kassis J, Lauffenburger DA, Turner T, Wells A. Tumor invasion as dysregulated cell motility. *Semin Cancer Biol*. 2001;11(2):105–117. doi:10.1006/scbi.2000.0362

45. Liu J, Qu J, Zhou W, et al. Syntenin-targeted peptide blocker inhibits progression of cancer cells. *Eur J Med Chem*. 2018;154:354–366. doi:10.1016/j.ejmech.2018.05.015

46. Yu Y, Liu M, Ng TT, et al. PDZ-reactive peptide activates ephrin-B reverse signaling and inhibits neuronal chemotaxis. *ACS Chem Biol*. 2016;11(1):149–158. doi:10.1021/acschembio.5b00889